Evaluation Method of the Sensors Errors in an Inertial Navigation System

TEODOR LUCIAN GRIGORIE
Avionics Department, University of Craiova
107 Decebal Street, 200440 Craiova
ROMANIA
lgrigore@elth.ucv.ro

NICOLAE JULA
Military Technical Academy
81-83 G. Cosbuc Blvd., Sector 5, Bucharest
ROMANIA
nicolae.jula@gmail.com

COSTIN CEPISCA
Electrical Engineering Faculty
University POLITEHNICA of Bucharest
313 Splaiul Independentei, Sector 6, Bucharest
ROMANIA
costin@wing.ro

CIPRIAN RĂCUCIU
Military Technical Academy
81-83 G. Cosbuc Blvd., Sector 5, Bucharest
ROMANIA
ciprian.racuciu@gmail.com

DAN RĂDUCANU
Military Technical Academy
81-83 G. Cosbuc Blvd., Sector 5, Bucharest
ROMANIA
dan.raducanu@gmail.com

Abstract: - The subject of this paper is a study of the influence of the inertial sensors errors on the position, speed and attitude of a bidimensional strap-down inertial navigation system in a horizontal plane. The MATLAB/SIMULINK models used for the acceleration and rotation sensors are based on the sensors data sheets and on the IEEE equivalent models for the inertial sensors. The models can be used in the numerical simulation of the strap-down inertial navigation system, close by real conditions from the point of view of the distortions suffered by the useful acceleration and rotation signals at the passing through any type of accelerometers or gyros desired to be implemented in the navigator. These models have the advantage to work independent from each of the sensors' errors and thus to study their influence on the inertial navigator.

Key-Words: - Sensors Models, Positioning Errors, Inertial Navigator, Inertial Sensors, Strap-Down.

1 Navigator Basic Equations

The position and the speed of a vehicle can be obtained through the direct integration of the general equation of the inertial navigation, relative to the navigation frame ([1], [2], [3], [4], [5]). In the case of the present navigation problem one chooses as a navigation frame the horizontal local frame $Ox_1y_1z_1$ (SOL). It can be approximated with an inertial frame considering the length and the specific of the mission. As a consequence, in the solving of the navigation problem there will be implied two reference frames: the horizontal local frame (SOL) and the vehicle frame (SV) (Fig. 1). The system being one of a bidimensional type in horizontal plane, will be considered just the x and y axis for the determination of the position and of the speed. This implies the using of a three inertial sensors in the navigator sensing system: two accelerometers installed on the x_v and y_v axis of the SV frame, and a gyro installed on the z_v axis of the same frame. We consider the following notations for the Fig. 1: $\vec{r}$ - the position

vector of the vehicle in the SOL frame, $\vec{v}$ - the speed of the vehicle relative to the SOL frame, v_{xv}, v_{yv} - the components of the vehicle speed on the SV frame axis, v_{xl}, v_{yl} - the components of the vehicle speed on the SOL frame axis, $\vec{\omega}$ - the angular speed of the vehicle relative to the SOL frame, ω_{zv} - the component of the $\vec{\omega}$ speed on the z_v axis of the SV frame (gyro reading), f_{xv}, f_{yv} - the components of the specific force $\vec{f}$ in the SV frame (accelerometric readings).

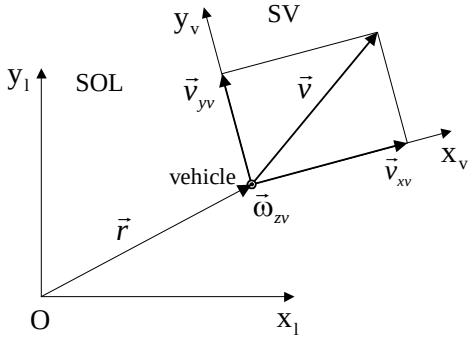

Fig. 1 Relative evolution of the SOL and SV frames

Because of the navigation in the horizontal plane, the output $\vec{f}$ of the accelerometer is not influenced by the gravitational field. So, the relation that expresses the connection between $\vec{f}$ and the kinematics acceleration $\vec{a}$ of the carrying vehicle is

$$\vec{f} = \vec{a} = \frac{\mathrm{d}\vec{v}}{\mathrm{d}t} + \vec{\omega} \times \vec{v}. \tag{1}$$

Projecting the equation (1) on the SV frame axis and retaining the equations on the x and y axis one obtains

$$\begin{aligned} f_{xv} &= \frac{\mathrm{d}v_{xv}}{\mathrm{d}t} + \omega_{zv} v_{yv}, \\ f_{yv} &= \frac{\mathrm{d}v_{yv}}{\mathrm{d}t} - \omega_{zv} v_{xv}. \end{aligned} \tag{2}$$

The numerical integration of the equations (2) provides the values of the vehicle speed components in the SV frame. Their transformation in the SOL frame is made using the relation ([3], [4], [6])

$$[v_{xl} \;\; v_{yl} \;\; v_{zl}]^T = R_v^l [v_{xv} \;\; v_{yv} \;\; v_{zv}]^T, \tag{3}$$

considering $v_{zv} = 0$. The determination of the R_l^v attitude matrix supposes the preliminary calculation of the yaw angle ψ, which is obtained through the numerical integration of the equation

$$\dot{\psi} = \omega_{zv}, \tag{4}$$

where ω_{zv} is the gyro reading. Also, in the calculus of the R_l^v matrix one particularize the roll and pitch angles with the values $\varphi = 0$ and $\theta = 0$.

The vehicle position is obtained through the numerical integration of the speed components in the SOL frame

$$\begin{aligned} x_l &= x_{l0} + \int_{t_{n-1}}^{t_n} v_{xl}\, dt, \\ y_l &= y_{l0} + \int_{t_{n-1}}^{t_n} v_{yl}\, dt, \end{aligned} \tag{5}$$

where x_{l0} and y_{l0} are the initial coordinates of the vehicle in the SOL frame.

Starting from the mathematical model previously presented one can deduce the analytical error model of the system, which will consider the influences of the inertial sensors errors on the vehicle attitude, position and speed. If we note with m the ideal value of a measurement, and with $\hat{m}$ its real value, offered by the measurement system, then the measurement error is calculated with the relation

$$\delta m = m - \hat{m}. \tag{6}$$

So, taking into account that for the bidimensional inertial navigator the accelerometric readings are f_{vx}, f_{yv}, and the gyro reading is ω_{zv}, it results the inertial sensors errors on the form

$$\begin{aligned} \delta f_{xv} &= f_{xv} - \hat{f}_{xv}, \\ \delta f_{yv} &= f_{yv} - \hat{f}_{yv}, \\ \delta \omega_{zv} &= \omega_{zv} - \hat{\omega}_{zv}. \end{aligned} \tag{7}$$

In the same manner are defined the errors of the attitude angle ψ, position (x_l, y_l), and speed (v_{xl}, v_{yl}) in SOL frame,

$$\begin{aligned} \delta\psi &= \psi - \hat{\psi}, \\ \delta x_l &= x_l - \hat{x}_l, \\ \delta y_l &= y_l - \hat{y}_l, \\ \delta v_{xl} &= v_{xl} - \hat{v}_{xl}, \\ \delta v_{yl} &= v_{yl} - \hat{v}_{yl}. \end{aligned} \tag{8}$$

Considering the equation (4), it results the differential equation for the error of the attitude angle determination

$$\delta\dot{\psi} = \delta\omega_{zv}. \tag{9}$$

Projecting the relation (1) on the SOL axes, one obtains

$$\left[\frac{\mathrm{d}\vec{v}}{\mathrm{d}t}\right]_l = [\vec{f}]_l - [\vec{\omega} \times \vec{v}]_l, \tag{10}$$

that is

$$\begin{aligned} \dot{v}_{xl} &= f_{xl} - (\vec{\omega} \times \vec{v})_{xl}, \\ \dot{v}_{yl} &= f_{yl} - (\vec{\omega} \times \vec{v})_{yl}. \end{aligned} \tag{11}$$

From the expressions (11), it results the differential equation of the vehicle speed errors under the form

$$\begin{aligned} \delta\dot{v}_{xl} &= \delta f_{xl} - \delta[(\vec{\omega} \times \vec{v})_{xl}], \\ \delta\dot{v}_{yl} &= \delta f_{yl} - \delta[(\vec{\omega} \times \vec{v})_{yl}]. \end{aligned} \tag{12}$$

Considering the particular form of the R_v^l attitude matrix for the bidimensional system, the accelerometric readings in the SOL frame are

$$\begin{bmatrix} f_{xl} \\ f_{yl} \\ f_{zl} \end{bmatrix} = R_v^l \cdot \begin{bmatrix} f_{xv} \\ f_{yv} \\ f_{zv} \end{bmatrix} = \begin{bmatrix} \cos\psi & -\sin\psi & 0 \\ \sin\psi & \cos\psi & 0 \\ 0 & 0 & 1 \end{bmatrix} \cdot \begin{bmatrix} f_{xv} \\ f_{yv} \\ f_{zv} \end{bmatrix}, \quad (13)$$

or

$$\begin{aligned} f_{xl} &= \cos\psi \cdot f_{xv} - \sin\psi \cdot f_{yv}, \\ f_{yl} &= \sin\psi \cdot f_{xv} + \cos\psi \cdot f_{yv}, \end{aligned} \quad (14)$$

from where it results

$$\begin{aligned} \delta f_{xl} &= \cos(\bar{\psi} + \delta\psi) \cdot (\bar{f}_{xv} + \delta f_{xv}) - \sin(\bar{\psi} + \delta\psi) \cdot \\ &\cdot (\bar{f}_{yv} + \delta f_{yv}) - \cos\bar{\psi} \cdot \bar{f}_{xv} + \sin\bar{\psi} \cdot \bar{f}_{yv}, \\ \delta f_{yl} &= \sin(\bar{\psi} + \delta\psi) \cdot (\bar{f}_{xv} + \delta f_{xv}) + \cos(\bar{\psi} + \delta\psi) \cdot \\ &\cdot (\bar{f}_{yv} + \delta f_{yv}) - \sin\bar{\psi} \cdot \bar{f}_{xv} - \cos\bar{\psi} \cdot \bar{f}_{yv}. \end{aligned} \quad (15)$$

Neglecting the products of the small infinites, one obtains

$$\begin{aligned} \delta f_{xl} &= \cos\bar{\psi} \cdot \delta f_{xv} - \sin\bar{\psi} \cdot \delta f_{yv} - \\ &- (\bar{f}_{xv} \sin\bar{\psi} + \bar{f}_{yv} \cos\bar{\psi}) \cdot \delta\psi, \\ \delta f_{yl} &= \sin\bar{\psi} \cdot \delta f_{xv} + \cos\bar{\psi} \cdot \delta f_{yv} + \\ &+ (\bar{f}_{xv} \cos\bar{\psi} - \bar{f}_{yv} \sin\bar{\psi}) \cdot \delta\psi. \end{aligned} \quad (16)$$

According with the relations (2) we have

$$\begin{aligned} (\vec{\omega} \times \vec{v})_{xv} &= \omega_{zv} \cdot v_{yv}, \\ (\vec{\omega} \times \vec{v})_{yv} &= -\omega_{zv} \cdot v_{xv}, \end{aligned} \quad (17)$$

and through successive transforming between frames, it results

$$\begin{aligned} (\vec{\omega} \times \vec{v})_{xl} &= \omega_{zv} \cdot v_{yl}, \\ (\vec{\omega} \times \vec{v})_{yl} &= -\omega_{zv} \cdot v_{xl}. \end{aligned} \quad (18)$$

The relations (18) imply

$$\begin{aligned} \delta[(\vec{\omega} \times \vec{v})_{xl}] &= (\bar{\omega}_{zv} + \delta\omega_{zv}) \cdot (\bar{v}_{yl} + \delta v_{yl}) - \bar{\omega}_{zl} \cdot \bar{v}_{yl}, \\ \delta[(\vec{\omega} \times \vec{v})_{yl}] &= -(\bar{\omega}_{zv} + \delta\omega_{zv}) \cdot (\bar{v}_{xl} + \delta v_{xl}) + \bar{\omega}_{zl} \cdot \bar{v}_{xl}, \end{aligned} \quad (19)$$

that is

$$\begin{aligned} \delta[(\vec{\omega} \times \vec{v})_{xl}] &= \bar{\omega}_{zv} \cdot \delta v_{yl} + \bar{v}_{yl} \cdot \delta\omega_{zv}, \\ \delta[(\vec{\omega} \times \vec{v})_{yl}] &= -\bar{\omega}_{zv} \cdot \delta v_{xl} - \bar{v}_{xl} \cdot \delta\omega_{zv}. \end{aligned} \quad (20)$$

So, resuming the relations (12), (16) and (20), the differential equations of the vehicle speed errors become

$$\begin{aligned} \delta\dot{v}_{xl} &= \cos\bar{\psi} \cdot \delta f_{xv} - \sin\bar{\psi} \cdot \delta f_{yv} - (\bar{f}_{xv} \cdot \sin\bar{\psi} + \\ &+ \bar{f}_{yv} \cdot \cos\bar{\psi}) \cdot \delta\psi - \bar{\omega}_{zv} \cdot \delta v_{yl} - \bar{v}_{yl} \cdot \delta\omega_{zv}, \\ \delta\dot{v}_{yl} &= \sin\bar{\psi} \cdot \delta f_{xv} + \cos\bar{\psi} \cdot \delta f_{yv} + (\bar{f}_{xv} \cdot \cos\bar{\psi} - \\ &- \bar{f}_{yv} \cdot \sin\bar{\psi}) \cdot \delta\psi + \bar{\omega}_{zv} \cdot \delta v_{xl} + \bar{v}_{xl} \cdot \delta\omega_{zv}. \end{aligned} \quad (21)$$

From the relations

$$\begin{aligned} \dot{x}_l &= v_{xl}, \\ \dot{y}_l &= v_{yl}, \end{aligned} \quad (22)$$

it results rapidly the differential equations of the vehicle position errors under the form

$$\begin{aligned} \delta\dot{x}_l &= \delta v_{xl}, \\ \delta\dot{y}_l &= \delta v_{yl}. \end{aligned} \quad (23)$$

So, in conclusion, the navigator error model is described by the equations

$$\begin{aligned} &\delta\dot{\psi} = \delta\omega_{zv}, \\ &\delta\dot{v}_{xl} = \cos\bar{\psi} \cdot \delta f_{xv} - \sin\bar{\psi} \cdot \delta f_{yv} - \bar{\omega}_{zv} \cdot \delta v_{yl} - \\ &\quad - \bar{v}_{yl} \cdot \delta\omega_{zv} - (\bar{f}_{xv} \cdot \sin\bar{\psi} + \bar{f}_{yv} \cdot \cos\bar{\psi}) \cdot \delta\psi, \\ &\delta\dot{v}_{yl} = \sin\bar{\psi} \cdot \delta f_{xv} + \cos\bar{\psi} \cdot \delta f_{yv} + \bar{\omega}_{zv} \cdot \delta v_{xl} + \\ &\quad + \bar{v}_{xl} \cdot \delta\omega_{zv} + (\bar{f}_{xv} \cdot \cos\bar{\psi} - \bar{f}_{yv} \cdot \sin\bar{\psi}) \cdot \delta\psi, \\ &\delta\dot{x}_l = \delta v_{xl}, \\ &\delta\dot{y}_l = \delta v_{yl}. \end{aligned} \quad (24)$$

The resulted model consists in a system of five coupled differential equations, and it contains five variables: one variable representing the determination error of the attitude angle ($\delta\psi$), two variables representing the determination errors of the vehicle speed relative to the SOL frame (δv_{xl}, δv_{yl}), and two variable representing the determination errors of the vehicle position relative to the SOL frame (δx_l, δy_l). The inputs of the model are the errors of the three inertial sensors used in the bidimensional strap-down inertial navigation system.

The analytical error model of the system includes the inertial sensors errors taken together. To study the individual influences of the sensors errors on the inertial navigator the error models for the sensors are conceived. The models cover the principal errors of the sensors.

2 Inertial Sensors Error Models

Starting from the parameters and from the errors of the rotation and acceleration sensors there were put up models for these, models standardized by the IEEE specialists for different categories of inertial sensors. The models established by the IEEE are used by the producers for the calibration operation of the sensors, and for the elaboration of theirs data sheets. Also, these models help the users in the compensation process of a great part of the sensors errors.

2.1 Accelerometers error models

From analyze of the IEEE standards referring to the accelerometers test procedures ([7], [8]) we concluded that for the accelerometers it is only one adopted model, used in high precision application. This one suppose the presence of the errors due to the bias, scale nonlinearity, misalignment of the input axis with respect to the output axis, cross-axis sensitivity, noise and to the erroneous calibration of the scale factor.

Such a model is described by the equation ([7], [8])

$$a_s = \frac{E}{K_1} = K_o + a_i + K_2 a_i^2 + K_3 a_i^3 + K_{ip} a_i a_p + \\ + K_{io} a_i a_o + \delta_o a_p - \delta_p a_o + \nu, \quad (25)$$

where a_s is the acceleration indicated by the accelerometer, E - sensor output, K_1 - scale factor, K_o - bias, K_2, K_3 - second-order, respectively third-order, nonlinearity coefficients, K_{ip}, K_{io} - cross-coupling coefficients, δ_o, δ_p - misalignments of the input axis with respect to the input reference axis about the output reference and pendulous reference axes, respectively, a_i, a_p, a_o - applied acceleration components along the positive input, pendulous, and reference axes, respectively, and ν - sensor noise.

Because the majority of the numerical simulations of strap-down inertial navigation systems, presented in the literature, suppose the application of clean acceleration and rotation signals to the system input, without errors and noises, the study of the navigation systems errors is made without taking into account the sensors errors. To put up a complex study for the navigation system, near by the real conditions, which will include the real errors of the used sensors, one can realize an equivalent model for the models described by the IEEE standards, a model which will consider the parameters from the sensors data sheets. So, one can opt for a model ([9]), which covers the main errors of the accelerometers, which can't be directly compensated

$$a = (a_i + Na_i + B + k_c a_c + \nu)\left(1 + \frac{\Delta K}{K}\right), \quad (26)$$

with a - output acceleration (disturbed signal), a_i - input acceleration, N - sensitivity axis misalignment, B - bias (deviation from zero at null input), a_c - cross -axis acceleration, k_c - cross-axis sensitivity, ν - sensor noise, K - scale factor, ΔK - scale factor error.

Starting from this simplified model it results a Matlab/Simulink model, based on the parameters variation limits offered by the sensors data sheets (Fig. 2.a). The model implements the observations in accordance with that in the data sheet a part of the parameters don't have a fixed value and vary arbitrary within an interval: cross-axis sensitivity is given throughout its maximum value k_c as a percent from a_c, the bias is given through its absolute maximum value B as a percent from span, scale factor error is given by its absolute maximum value ΔK as a percent from K, and noise is given by the maximum value of its density.

Grouping the schema in Fig. 2.a it results the block in Fig. 2.b, which has as inputs the acceleration a_i applied along of the sensitivity axis and the acceleration a_c applied in a perpendicular plane, and as output the disturbed acceleration a.

The model was built for a few acceleration sensors, realized in MEMS (Micro-Electro-Mechanical Systems), MOEMS (Micro-Opto-Electro-Mechanical Systems) technologies or in classical approach. The change of the sensor type that will be used in simulations is made using the interface in Fig. 3. In addition, the interface allows the setting of the model, by the user, in a custom variant, with the manual inserting of the parameters in the characteristic fields. The model can be used in the numerical simulation of the strap-down inertial navigation system, close by real conditions from the point of view of the distortions suffered by the useful acceleration signal at the passing through any type of accelerometer desired to be implemented in navigator.

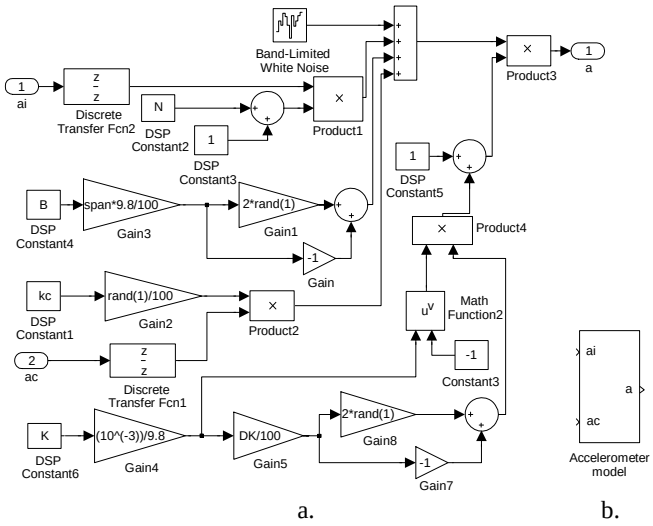

a. b.

Fig. 2 Simulink error model for accelerometers

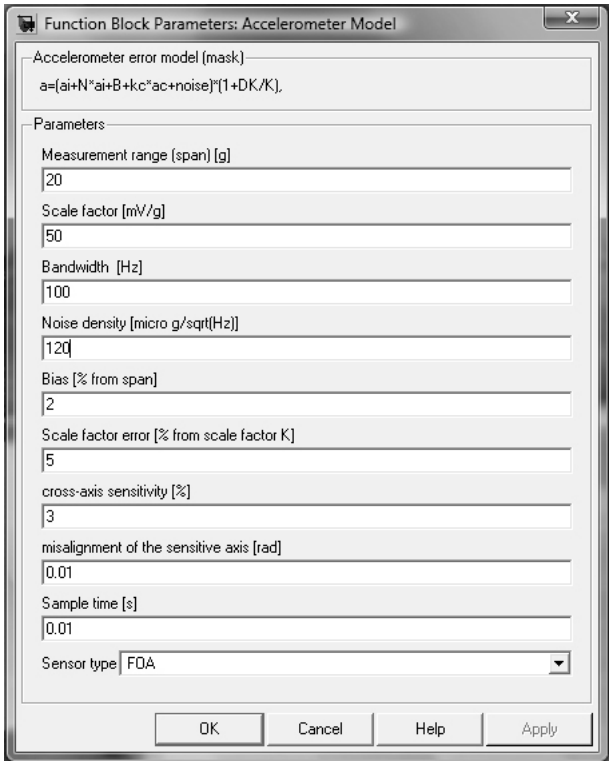

Fig. 3 The interface of the accelerometers error model

2.2 Gyros error models

The appearance of the optoelectronic gyros and the increase of theirs performances over the performances of the mechanical gyros led to their use at the large-seal in the high precision strap-down inertial navigation systems and to the gradual renunciation at the use of mechanical gyros in these systems. Therefore, in the '90 years the IEEE specialists were resorted to the standardization of the testing procedures for the main types of such gyros (laser gyros [10] and interferometric fibber optic gyros [11]). The actual trend in the inertial navigation systems miniaturization had on the rotation sensors the same impact like in the acceleration sensors case. Thus, the MEMS technology was strongly developed in this direction, resulting miniaturized gyros with the functioning principle based on the Coriolis forces due to the rotation movement that must be detected. An IEEE recent standard ([12]) specifies the test procedures for Coriolis vibratory gyroscopes.

In according with the standards for the optoelectronic rotation sensors ([10], [11]), if the sensor output is digital then the gyro error model can be described by a relation of the form

$$S_0(\Delta N/\Delta t) = [I + E + D][1 + 10^{-6}\varepsilon_K]^{-1}, \tag{27}$$

with S_0 the nominal scale factor expressed in $''/\text{pulse}$ and $\Delta N/\Delta t$ the output pulse rate expressed in pulse/s. If the sensor output is analogue, the IEEE model has the equation

$$S_0 U = [I + E + D][1 + 10^{-6}\varepsilon_K]^{-1}, \tag{28}$$

where S_0 the nominal scale factor expressed in $(^o/\text{h})/\text{V}$, and U is the analogue output voltage expressed in V. In the relations (27) and (28) I is inertial input terms $(^o/\text{h})$, E - environmentally sensitive terms $(^o/\text{h})$, D the drift terms $(^o/\text{h})$ and ε_K is the scale factor error terms (in ppm). The expressions for all four physical quantities are ([10], [11])

$$\begin{aligned} I &= \omega_{IRA} + \omega_{XRA}\sin\theta_X - \omega_{YRA}\sin\theta_Y, \\ E &= D_T\Delta T + D_{\dot T}(\mathrm{d}T/\mathrm{d}t) + \overline{D}_{\nabla\dot{\overline{T}}}\cdot[\mathrm{d}(\nabla\overline{T})/\mathrm{d}t], \\ D &= D_F + D_R, \\ \varepsilon_K &= \varepsilon_T\Delta T + f(I), \end{aligned} \tag{29}$$

where $\omega_{IRA}, \omega_{XRA}, \omega_{YRA}$ are the components of the inertial input rate resolved into the gyro reference coordinate frame (*IRA* – input axis), θ_X, θ_Y - misalignment of the proper input axis of the sensor (*IA*) and the axes *XRA* and *YRA*, $D_T\Delta T$ - drift rate attributable to a change in temperature ΔT, D_T - drift rate temperature sensitivity coefficient, $D_{\dot T}(\mathrm{d}T/\mathrm{d}t)$ - drift rate attributable to a temperature ramp, $D_{\dot T}$ - coefficient of the temperature-ramp drift-rate sensitivity, $\overline{D}_{\nabla\dot{\overline{T}}}\cdot[\mathrm{d}(\nabla\overline{T})/\mathrm{d}t]$ - drift rate attributable to a time-varying temperature-gradient $\mathrm{d}(\nabla\overline{T})/\mathrm{d}t$, $\overline{D}_{\nabla\dot{\overline{T}}}$ - coefficient vector of the time-varying temperature-gradient drift-rate sensitivity, D_F - bias, D_R - random drift rate (equivalent with a noise), $\varepsilon_T\Delta T$ - scale factor error attributable to a change in temperature ΔT, and $f(I)$ is the scale factor errors dependent on input rate.

The error models for the electromechanical and electronomechanical gyro sensors ([12]) have similar expressions with relations (27) and (28) in case of digital or analogue output. For frequency output, the model can be expressed as follows

$$S_0 F = [I + E + D][1 + 10^{-6}\varepsilon_K]^{-1}, \tag{30}$$

and for ratiometric output, with the relation

$$\begin{aligned} S_0(V_{ref}/Vp)U = [I + E + D]\cdot[1 + 10^{-6}\varepsilon_K]^{-1}\cdot \\ \cdot[1 + K_r(V_{ref}/V_p)], \end{aligned} \tag{31}$$

where F is frequency output (Hz), V_{ref} - voltage at which the nominal scale factor is determined, V_p - power supply voltage and K_r - ratiometric error coefficient. The only one difference comparatively with the optoelectronic sensors model, from the point of view of the equations (5), is the presence in the expressions of E and ε_K of the additionally terms $D_a a$, respectively $S_a a$. They show that E and ε_K are dependent by the acceleration a, applied along any given axis, with the sensitivities D_a, respectively S_a.

Starting from the same reason like in the accelerometers case, to create an equivalent model for the IEEE models, which will consider the parameters from the sensors data sheets and will permit the putting up of strap-down inertial navigation systems studies near by the real conditions, one can opt for the model described by the relation [9]

$$\omega = (\omega_i + S\cdot a_r + B + \nu)\left(1 + \frac{\Delta K}{K}\right), \tag{32}$$

with ω - output angular speed (disturbed signal), ω_i - input angular speed, S - sensitivity at the acceleration a_r applied by an arbitrary direction, B - bias, K - scale factor, ΔK - scale factor error, and ν - sensor noise.

On the basis of the model described by the equation (32) it results a Matlab/Simulink model, which considers the parameters variation limits offered by the sensors data sheets (Fig. 4.a). Like in the acceleration sensors case, the model has in view that the bias is given through its absolute maximum value *B* as a percent from span, scale factor error is given by its absolute maximum value ΔK as a percent from *K*, and noise is given by the maximum value of its density.

The resulted block from the grouping of the scheme in Fig. 4.a is presented in Fig. 4.b. He has as inputs the

angular speed ω_i applied along of sensitivity axis of the sensor and the acceleration a_r considered to be the resultant non-disturbed acceleration signal (the resultant of the accelerations applied on the three directions to the accelerometric triad from a standard strap-down inertial system), and as output the disturbed angular speed ω.

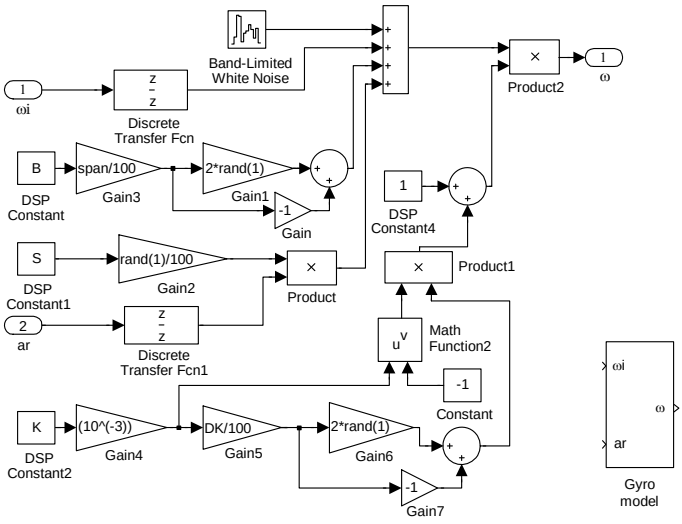

a. b.

Fig. 4 Simulink error model for gyros

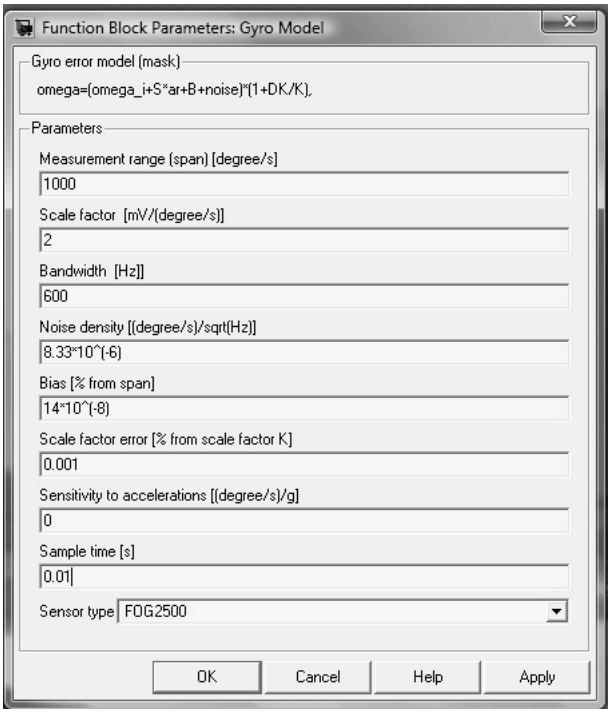

Fig. 5 The interface of the gyros error model

The model was built for a few gyro sensors, electronic and optoelectronic, realized in MEMS technology or in classical approach. The change of the sensor type that will be used in simulations is made using the interface in Fig. 5. In addition, the interface allows the setting of the model, by the user, in a custom variant, with the manual inserting of the parameters in the characteristic fields.
The resulted models can be used in the numerical simulation of the strap-down inertial navigation system, near by the real conditions from the point of view of the deformations of the useful signal that undergoes any type of accelerometer or gyro meant to be implemented in the navigator.

3 Study of the Influences of the Inertial Sensors Errors on the Navigator Errors

The study will be realized in two phases: the validation of the analytical error model of the system and the evaluation of the influence level in the positioning errors for principal errors of the inertial sensors.

3.1 The validation of the navigator analytical error model

Starting from the navigator equations and from the theoretical algorithm that solves the presented navigation problem it results the Matlab/Simulink model in Fig. 6.a. The block „SV in SOL" models the transformation from the SV frame coordinates in the SOL frame coordinates. Grouping the schema in Fig. 6.a one obtains the block in Fig. 6.b. Its inputs are the gyro reading ω_{zv} and the accelerometric readings f_{xv}, f_{yv}, and its outputs are the attitude of the vehicle, expressed by the yaw angle ψ, the position in the SOL frame given by the components x_l and y_l, and the speed relative to the SOL frame, given by the components v_{xl} and v_{yl}.

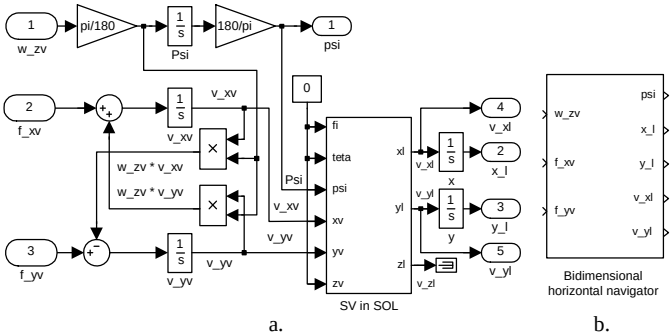

a. b.

Fig. 6 Navigator Matlab/Simulink model

For the sensors errors influence study on the navigation algorithm one uses the models in Fig. 2 and Fig. 4, and the navigator model in Fig. 6. With these models it results the validation Simulink model in Fig. 7. The "IDEAL" and "REAL" blocks are blocks by the form in Fig. 6.b, its inputs being acceleration and rotation signals non-disturbed by the inertial sensors errors, respectively disturbed by the inertial sensors errors. The blocks

"Acc" and "Gyro", from the input of the simulation model, are error models of the accelerometers and of the gyros. Their outputs are applied to the "REAL" block. The values of the input constants are considered to be ideal signals, non-disturbed by the inertial sensors errors, these being applied to the "IDEAL" block. The evaluation of the errors induced in the navigator by the inertial sensors is put up by means of the calculation of the differences between the quantities obtained to the outputs of the "IDEAL" and "REAL" blocks for position, speed and attitude. For study we have chosen two capacitive accelerometric sensors and a gyro laser, having the parameters in Table 1 and the $\delta\omega_{zv}$, δf_{xv}, δf_{yv} errors characteristics in Fig. 8.

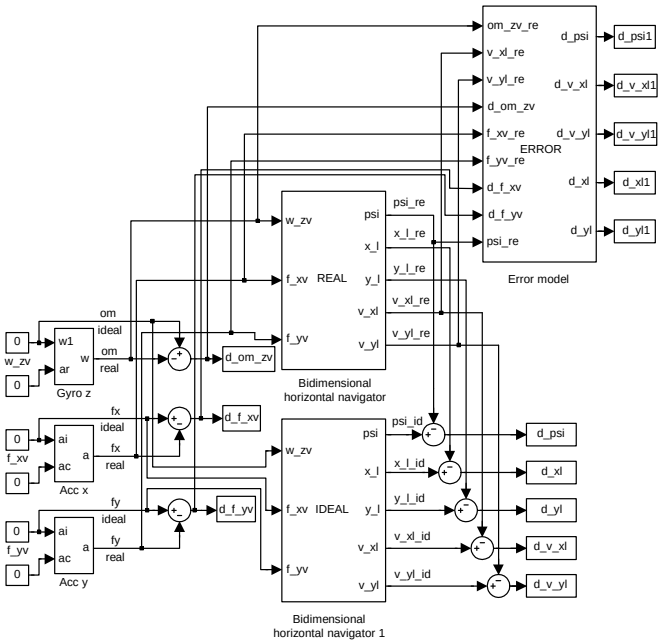

Fig. 7 Simulation model

The validation of the navigator error model is realized through the comparison of the differences between the quantities obtained to the outputs of the "IDEAL" and "REAL" blocks with the outputs of the "ERROR" block. In Fig. 9 are represented the errors of the solution of navigation for 10 s simulation time and null navigator inputs. First column contains the differences between the quantities obtained to the outputs of the "IDEAL" and "REAL" blocks, and the second column the outputs of the "ERROR" block.

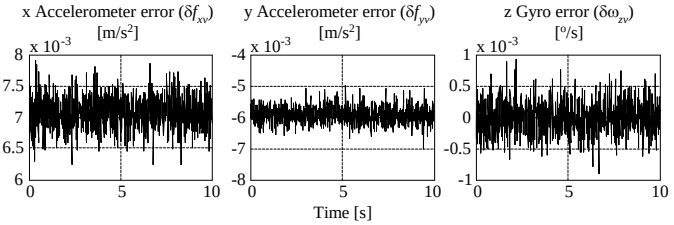

Analyzing the curves in Fig. 9, one can conclude that the allures of the graphical characteristics in the first column are identical with the allures of the graphical characteristics in the second column. So, the error model described by the equations (24) characterizes precisely the deviations from the ideal value for the attitude angle, position and speed (relative to the SOL frame), under the influence of the inertial sensors errors used in navigator.

Table 1 Parameters of the inertial sensors used in numerical simulations

Sensor	Bias	Scale factor error	Noise density
x Accelerometer	$-7{,}0928 \cdot 10^{-3}$ m/s^2	0,2%	70 μg/$\sqrt{\text{Hz}}$
y Accelerometer	$5{,}9094 \cdot 10^{-3}$ m/s^2	0,28%	70 μg/$\sqrt{\text{Hz}}$
z Gyro	$4{,}2 \cdot 10^{-6}$ ^{o}/s	$-3{,}12 \cdot 10^{-4}$ %	$6{,}6 \cdot 10^{-4}$ (^{o}/s)/$\sqrt{\text{Hz}}$

Fig. 8 Inertial sensors errors

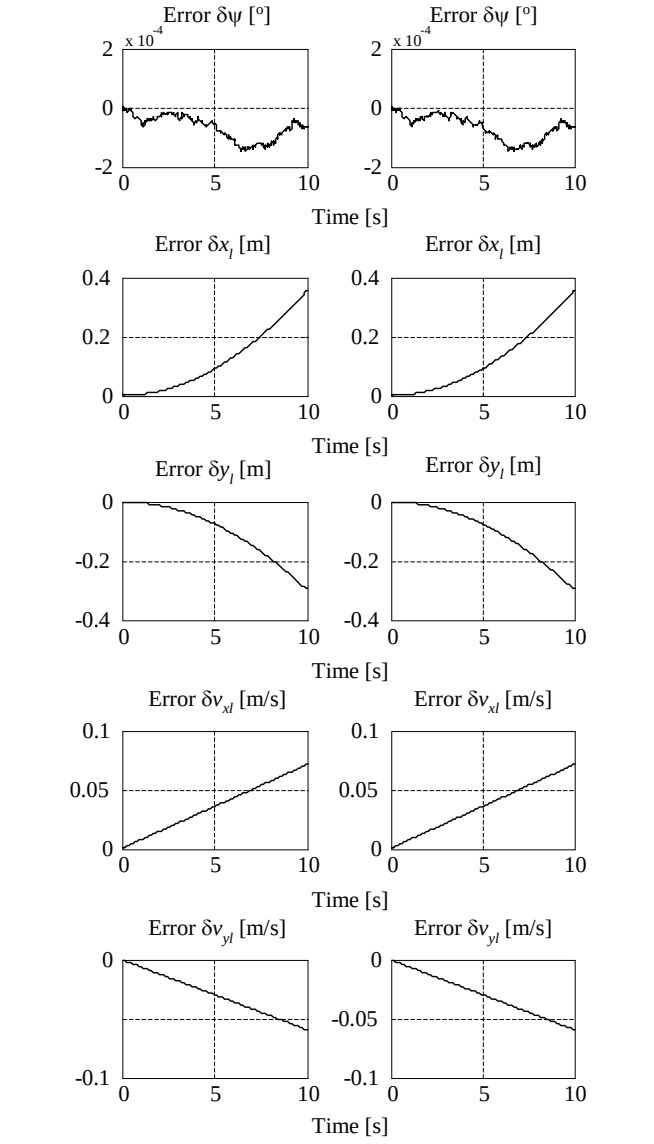

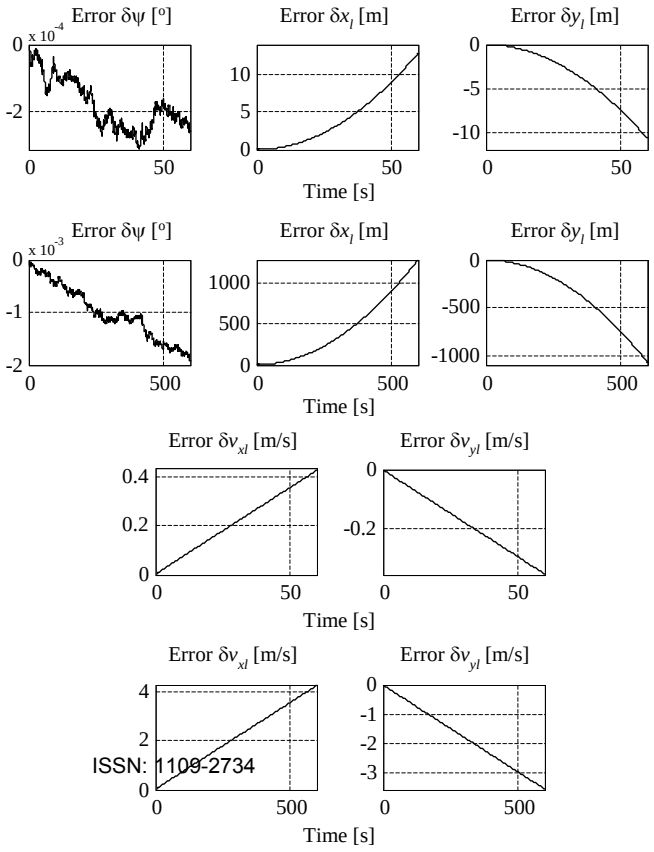

Fig. 9 Validation of the analytical error model

3.2 The evaluation of the influence level in the positioning errors for principal errors of the inertial sensors

In the first phase numerical simulations are put up for null inputs and different times (10 s, 1 min, 2 min, 3 min, 4 min, 5 min, 10 min, 100 min) resulting in the absolute maximal values of the attitude, position and speed errors in Table 2 and the graphic characteristics of the errors in Fig. 10 (for 1 min and 10 min times).

Fig. 10 Navigator errors for 1 min, respectively 10 min, simulation time

Table 2 Absolute maximal values of the navigator errors for different simulation times

Simulation time	Attitude angle error [°]	Positioning errors [m]		Speed errors [m/s]	
	$\delta\psi$	δx_l	δy_l	δv_{xl}	δv_{yl}
10 s	$1.5037 \cdot 10^{-4}$	0.3538	0.2961	0.0708	0.0592
1 min	$3.0655 \cdot 10^{-4}$	12.7392	10.6631	0.4246	0.3554
2 min	$5.2050 \cdot 10^{-4}$	50.9485	42.6555	0.8491	0.7109
3 min	$7.0850 \cdot 10^{-4}$	114.6377	95.9688	1.2737	1.0663
4 min	$9.7507 \cdot 10^{-4}$	203.7982	170.6138	1.6983	1.4218
5 min	$1.2275 \cdot 10^{-3}$	318.4362	266.6034	2.1227	1.7778
10 min	$1.9276 \cdot 10^{-3}$	1273.7258	1066.6043	4.2456	3.5553
100 min	$2.5151 \cdot 10^{-2}$	127427.062	106650.316	42.4851	35.5453

Further on, one made simulations with 1 min simulation time for different cases in that occur or not the values of certain categories of errors which influence the inertial sensors, with the goal to find out these weights in the final errors of the inertial navigator. Keeping the previous initial conditions and the sensors noise, one considers the following variants during the simulation: bias and scale factor error null for accelerometers and for gyro (Fig. 11), the accelerometers bias non-null and the others errors null (Fig. 12), the accelerometers scale factor error non-null and the others errors null (Fig. 13), the accelerometers with all errors non-null and the gyro with all errors null, the gyro bias non-null and the others errors null (Fig. 14), the gyro scale factor error non-null and the others errors null (Fig. 15), the gyro with all errors non-null and the accelerometers with all errors null. It results the absolute maximum values for the attitude, position and speed in Table 3.

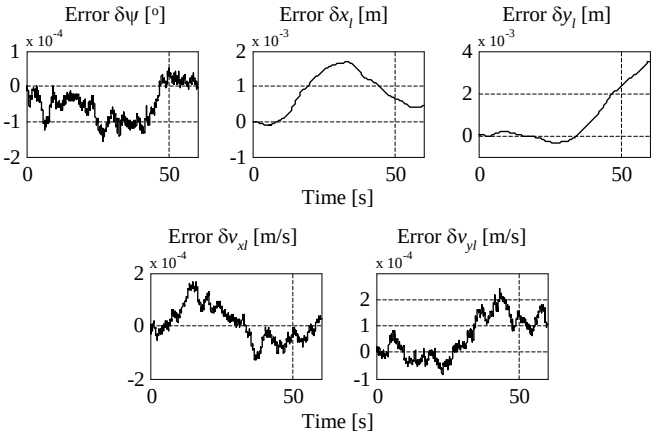

Fig. 11 Output errors for the sensors noise only

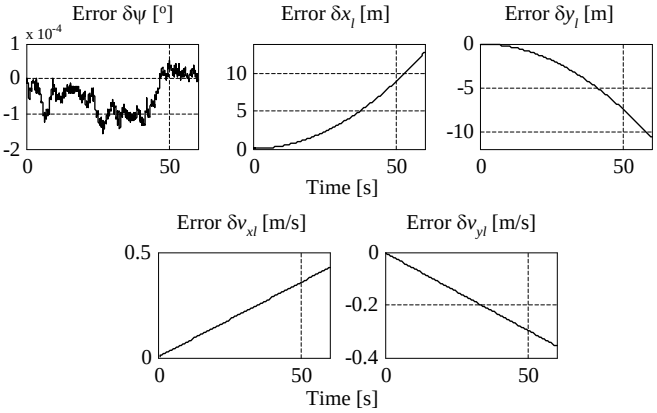

Fig. 12 Output errors for $B_{Acc} \neq 0$

Table 3 Absolute maximal values of the navigator errors for different inertial sensors errors

Sensors errors	Attitude angle error [°]	Positioning errors [m]		Speed errors [m/s]	
	$\delta\psi$	δx_l	δy_l	δv_{xl}	δv_{yl}
Noise only	$1.5648 \cdot 10^{-4}$	0.0016	0.0035	$1.6518 \cdot 10^{-4}$	$2.4055 \cdot 10^{-4}$
$B_{Acc} \neq 0$	$1.5648 \cdot 10^{-4}$	12.7647	10.6333	0.4255	0.3544
$\Delta K_{Acc} \neq 0$	$1.5648 \cdot 10^{-4}$	0.0016	0.0035	$1.6485 \cdot 10^{-4}$	$2.4122 \cdot 10^{-4}$
$B_{Acc} \neq 0$ & $\Delta K_{Acc} \neq 0$	$1.5648 \cdot 10^{-4}$	12.7392	10.6631	0.4246	0.3554
$B_{Gyro} \neq 0$	$3.0655 \cdot 10^{-4}$	0.0016	0.0035	$1.6518 \cdot 10^{-4}$	$2.4055 \cdot 10^{-4}$
$\Delta K_{Gyro} \neq 0$	$1.5648 \cdot 10^{-4}$	0.0016	0.0035	$1.6518 \cdot 10^{-4}$	$2.4055 \cdot 10^{-4}$
$B_{Gyro} \neq 0$ & $\Delta K_{Gyro} \neq 0$	$3.0655 \cdot 10^{-4}$	0.0016	0.0035	$1.6518 \cdot 10^{-4}$	$2.4055 \cdot 10^{-4}$
All errors	$3.0655 \cdot 10^{-4}$	12.7392	10.6631	0.4246	0.3554

non-null					

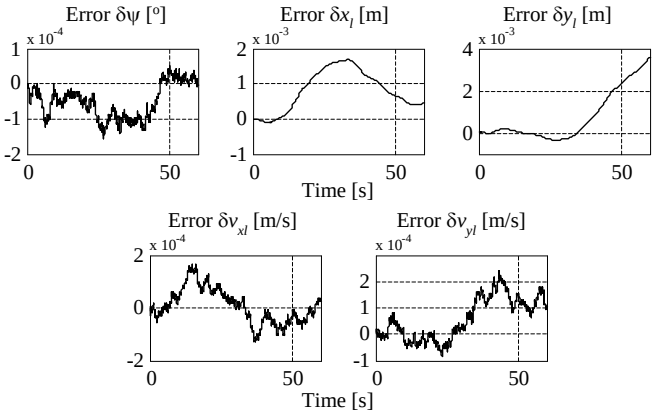

Fig. 13 Output errors for $\Delta K_{Acc} \neq 0$

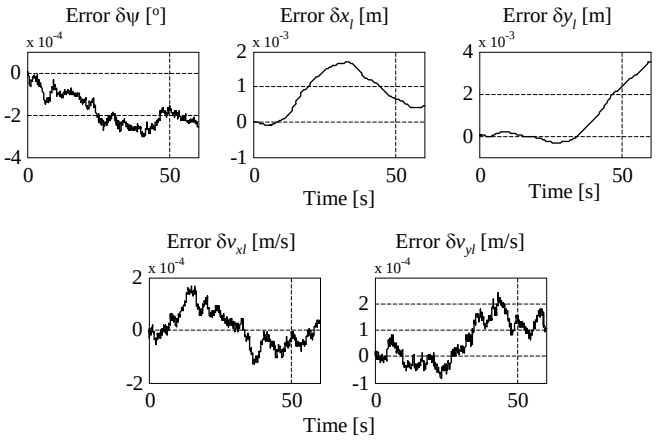

Fig. 14 Output errors for $B_{Gyro} \neq 0$

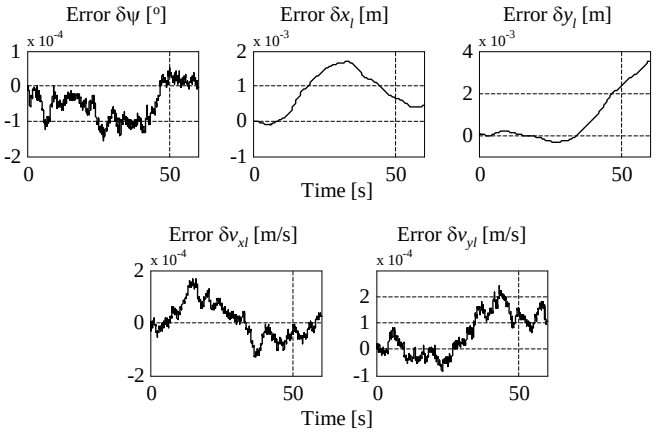

Fig. 15 Output errors for $\Delta K_{Gyro} \neq 0$

4. Conclusions

Analyzing the graphic characteristics in Fig. 10 and the numerical results in Table 2 one can conclude the follows: errors of attitude angle are maintained in reasonable limits even after 100 min (the maximal value is 0.02515^{o}); position errors are divergent on both

channels, having an approximate parabolic carriage; speed errors have, also, a divergent character on both channels with an approximate linear carriage.

From Table 2 it results that, for the case in which the vehicle navigator remains only with the inertial system (without the assistant system), in choosing the configuration for the sensors system, this can be used for 3 minutes maximum time with position errors until 114.6377 m on the x channel and until 95.9688 m on the y channel. Over the limit of the 3 minutes the errors increase on both channels, after 10 minutes becoming 1273.7258 m on the x channel and 1066.6043 m on the y channel. So, the navigation system in actual configuration can be used for 3 minutes maximum time in complete, and just with the attitude angle over the 3 minutes time.

According with the graphic characteristics in Fig. 11 ÷ Fig. 15 and with numerical results in Table 3, the accelerometers scale factor errors and biases have null weights in the increase of the attitude angle error (the same carriages in Fig. 11 ÷ Fig. 13). Also, the gyro bias and scale factor error influence on the positioning and speed errors is almost negligible (from the nine decimal away at the absolute maximal values and carriages almost identical in Fig. 12 ÷ Fig. 15). So, for the studied navigator and for the chosen architecture of the inertial sensors system, on can conclude that the attitude channel can be completely separated from the position and speed channels from the point of view of the errors. Practically, the gyro influences only the attitude angle, and the accelerometers influence only the position and speed.

Analyzing the gyro influence in the attitude channel one observes that the great weight in the final error is the noise weight (51.047%), being followed by the bias in an almost equal proportion. The scale factor error of the gyro has a negligible influence in the final error of the attitude angle (≈0.000159%).

For the accelerometers influences in the position and speed channels one observes that the decisive weights in the final errors is the biases weights (over the 99% from the error value), being followed by the noise (value under 0.015%). The accelerometers scale factor errors have a negligible influence in the final errors of the position and of the speed (value under 0.00003%).

In conclusion, the most significant errors for this application is the bias and the noise, that for the gyro influence the attitude angle in almost equals proportions, and for the accelerometers influence the position and speed channels in proportions over 99%, respectively under 0.0015%.

The weights of the sensors errors are in majority determined by the quality of the chosen sensors. As an example, for the accelerometers the bias has great values for the noise values smaller than the noise values for the gyro.

Another observation is tied by the errors combination. One can observe that is obtained an increase or a decrease of the absolute maximal values of the navigator errors in the general case as against the particulars cases, when are studied the influences of each error of the inertial sensors. This combination can be explained booth from the positive and negative values of the sensors parameters (see Table 1), and from the evolutions in the positive or negative zones of the error characteristics in Fig. 11 ÷ Fig. 15.

Also, the present study is very important from the point of view of the fact that it offers an evaluation method for the errors induced by the inertial sensor in a strap-down inertial navigation system just on the base of the sensors data sheets. This is a very delicate step for the navigator designers in the inertial sensors choice phase.

References:

[1] R.M. Rogers, *Applied Mathematics in Integrated Navigation Systems.* AIAA, 2003.

[2] A.B. Chatfield, A.B. *Fundamentals of High Accuracy Inertial Navigation*. AIAA, 1997.

[3] J. Farrell, M. Barth, *The Global Positioning System and Inertial Navigation*. McGraw-Hill, 1999.

[4] T.L. Grigorie, *Sisteme de Navigație Inerțială Strap-Down. Studii de Optimizare*. Editura SITECH, Craiova, Romania, 2007. ISBN: 978-973-746-723-2.

[5] R., Lungu, M., Lungu, N., Jula, C., Cepisca, *Models identification and adaptive control of the flying objects using neural networks*, Proceedings of WSEAS Conferences, Arcachon, Oct. 13-15, 2007.

[6] O.S. Salychev, *Inertial Systems in Navigation and Geophysics*. Bauman MSTU Press, 1998.

[7] IEEE Std. 1293-1998, *IEEE Standard Specification Format Guide and Test Procedure for Linear, Single-Axis, Nongyroscopic Accelerometers*, Published by IEEE, New York, USA, 16 April, 1999.

[8] IEEE Std. 836-1991, *IEEE Recommended Practice for Precision Centrifuge Testing of Linear Accelerometers*, Published by IEEE, New York, USA, June 15, 1992.

[9] R. Lungu, T.L. Grigorie, *Traductoare Accelerometrice şi Girometrice*. Editura SITECH, Craiova, Romania, 2005. ISBN: 973-657-777-5.

[10] IEEE Std. 647-1995, *IEEE Standard Specification Format Guide and Test Procedure for Single-Axis Laser Gyros*, Published by IEEE, New York, USA, September 21, 1995.

[11] IEEE Std. 952-1997, *IEEE Standard Specification Format Guide and Test Procedure for Single-Axis Interferometric Fiber Optic Gyros*, Published by IEEE, New York, USA, September 16, 1997.

[12] IEEE Std. 1431-2004, *IEEE Standard Specification Format Guide and Test Procedure for Coriolis Vibratory*

Gyros, Published by IEEE, New York, USA, December 20, 2004.
[13] H., Andrei, C., Cepisca, G., Chicco, *LabVIEW measurements in steady state nonsinusoidal regime*, WSEAS Transactions on Circuits and Systems, Issue 11, volume 5, November 2006, pp. 1682.
[14] M., Lungu, R., Lungu, N., Jula, C., Cepisca, M., Calbureanu, *Optimal command of aircrafts move using a reducer order observer*, Proceedings of the 9th WSEAS International Conference on Automation and Information (ICAI 08), Bucharest, Romania, June 24-26, 2008, pp. 332-337.